Small-angle neutron scattering studies of diffusion in bulk polymers: Experimental procedures

2 AUTHORS, INCLUDING:

Jwo-Huei Jou
National Tsing Hua University

158 PUBLICATIONS   **2,062** CITATIONS

Small-Angle Neutron Scattering Studies of Diffusion in Bulk Polymers: Experimental Procedures[†]

J. E. Anderson*

Research Staff, Ford Motor Company, Dearborn, Michigan 48121

J.-H. Jou[‡]

Department of Nuclear Engineering and Macromolecular Science and Engineering, The University of Michigan, Ann Arbor, Michigan 48109. Received November 17, 1986

ABSTRACT: This research addresses experimental issues arising in SANS diffusion studies of bulk polymers. Sample preparation, annealing protocols, reproducibility of replicate samples, data reduction, and analysis procedures are considered. Experimental SANS data for 68 000 MW polystyrene are examined in detail. These data were obtained on specimens containing 50 wt % protonated and deuteriated polymer. The initial specimens were heterogeneous, containing domains of protonated and deuteriated polystyrene. Heterogeneities were destroyed, by interdiffusion, during sample annealing at 130 °C. SANS results, made as a function of annealing time, were analyzed to characterize diffusion. This analysis yielded diffusion coefficients that appeared to increase with scattering angle: values between 9×10^{-16} and 1.8×10^{-15} cm²/s were obtained over the range $Q = (4.0–8.0) \times 10^5$ cm⁻¹. We attribute this apparent Q dependence to instrumental effects, specifically, to "smearing" of experimental data. Simulation of scattering results, using an appropriate "smearing" function, generates values that match experiment. Simulation indicates that "smearing" has a minimal effect on diffusion coefficients measured at higher scattering angles. A *constant* (Q-independent) value $D = 1.8 \times 10^{-15}$ cm²/s is suggested for 68 000 MW polystyrene at 130 °C.

Introduction

This report concerns small-angle neutron scattering (SANS) methods for studies of diffusion in bulk polymers. It deals with experimental issues and techniques. In particular, our results validate a theoretical analysis of polymer diffusion/SANS developed by Summerfield and Ullman.[1] An experimental diffusion coefficient of 1.8×10^{-15} cm²/s was determined for bulk polystyrene of 68 000 MW at 130 °C. This is a resonable extrapolation of larger diffusion coefficients reported by Antonietti et al.,[2] by Klein et al.,[3] and by Kramer et al.[4] for polystyrene of different molecular weights and at different temperatures. We have used SANS/diffusion experiments to investigate translational motion in polystyrene at temperatures near T_g, where diffusion coefficients are typically 10^{-15}–10^{-17} cm²/s. These data will be reported in a future paper.

Diffusion experiments based on scattering originated in the 1940 X-ray study of DuMond and Youtz[5] of the Au–Cu system. Numerous scattering/diffusion studies on binary metal systems have been reported since then.[6–8] The experiments view translational motion over dimensions characteristic of X-ray and neutron scattering, i.e., lengths of 10^{-8} to 10^{-5} cm. It follows, from the relation $D = \langle x^2 \rangle / 2t$, that scattering methods can examine *extremely* slow motions during convenient laboratory time scales and measure, e.g., $D = (1–10) \times 10^{-20}$ cm²/s.[5] Moreover, scattering experiments can probe non-Fickian effects associated with motion over small distances.[6–8] Measurements may be made at constant scattering angle and/or at constant diffusion time. This permits studies of space-dependent (Q-dependent) and time-dependent diffusion.

Experiments involve heterogeneous (nonequilibrium) specimens that are stable with respect to diffusive intermixing at low temperatures where the samples are stored and where scattering measurements are carried out. The heterogeneities are destroyed, by molecular interdiffusion, at high temperatures. Experiments start by measuring scattering from an initial, heterogeneous specimen. Sub-

sequently, this specimen is annealed at an elevated temperature for a known time interval and then cooled to ambient temperature where scattering is measured again. Diffusion coefficients are obtained from analysis of scattering changes with annealing time.

Molecular diffusion has distinctly different effects on low-Q and high-Q scattering (Figure 1). Low-angle scattering[1,8] *decreases* toward its equilibrium value as $\exp[-2DQ^2t]$, independent of the initial heterogeneity distribution. Higher angle scattering *increases* toward its equilibrium value with sample annealing. This scattering increase involves a spatial integral of time-dependent radial correlation function; consequently, it depends on the initial heterogeneity distribution. Increasing and decreasing SANS regions are *not* independent of one another. Rather, they reflect the invariance of I_T, the integral of the scattering intensity over all angles[8]

$$I_T = \int_0^\infty Q^2 I(Q) \, dQ = \beta_0 \int_0^\infty [C(R) - \phi]^2 \, d^3R = \text{constant}$$

In this expression, $Q = (4\pi/\lambda) \sin (\theta/2)$, $C(R)$ is the volume fraction of deuteriated polymer at position R, ϕ is the average volume fraction deuteriated polymer; β_0 is a proportionality constant, and $I(Q)$ is the scattering intensity.

Scattering/diffusion studies of polymers are more complicated than diffusion studies of metals (Figure 1). If one works in the low-Q region, scattering from binary metals effectively decays to zero at equilibrium, i.e., at very long annealing times, because the components become mixed over monomeric distances. With metals, increases in SANS with annealing time occur only at angles well separated from the Q region of scattering decay. This clean division does not occur for polymers, where macromolecular dimensions cause overlap between growing and decaying portions of scattering curves. A recent calculation by Summerfield and Ullman[1] provides a mechanism for disentangling growth and decay of scattering contributions during polymer annealing/interdiffusion.

Scattering/diffusion methods have been applied only recently to bulk polymer systems. Bartels et al.[9] studied melts containing protonated and deuteriated polybutadiene and measured the increase in high-Q neutron scattering with annealing time. Experiments in the
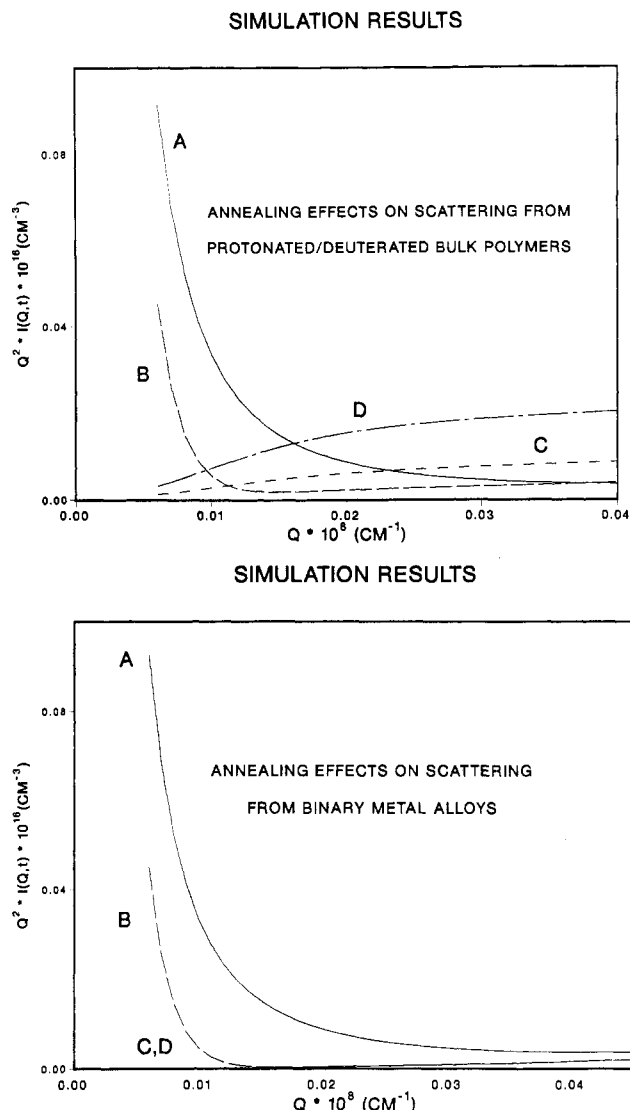
SIMULATION RESULTS

SIMULATION RESULTS

Figure 1. Schematic representation of the SANS diffusion experiment. Computer simulation was used to generate scattering intensities, $I(Q)$, as a function of annealing time. Curves (A) represent scattering from heterogeneous starting materials plotted as $Q^2 I(Q)$ vs. Q. Curves (B) and (C) correspond to specimens annealed for intermediate times, curves (D), to homogeneous (fully annealed) specimens. The upper and lower graphs contrast SANS diffusion experiments on polymeric and metallic systems. Macromolecular dimensions produce substantial scattering from homogeneous polymer samples. This scattering contribution is small in the heterogeneous starting materials but increases with polymer interdiffusion, i.e., with annealing time. In binary metals, increased scattering during annealing occurs only at Q values larger than those shown here.

high-angle region minimize the overlap problem, outlined above; however, they require accurate knowledge of the initial distribution of protonated and deuteriated polymers. X-ray measurements were employed by Hashimoto et al.[10] to follow the changes in low-angle scattering of block copolymers during demixing.

Experimental Procedure

Sample Preparation. The specimens used in this study contained 50 wt % protonated polystyrene (HPS) in deuteriated polystyrene (DPS). HPS/DPS matched molecular weight samples were prepared from monodisperse homopolymers [$M_w/M_n < 1.06$] having M_w's of 68 000 and 110 000. Concentrated solutions of HPS in HPS/benzene and DPS/benzene were emulsified in an aqueous solution containing sodium lauryl sulfate. Ultrasonic agitation was used. The two HPS and DPS emulsions then were mixed together, freeze-dried to remove solvent, and washed with hot

distilled water to remove emulsifier. The resulting wet powder was dried under vacuum at 65 °C until constant weight was obtained.

Dimensions of the loose and irregular segregated clusters are estimated to range between 1.2×10^{-5} and 10×10^{-5} cm on the basis of SEM studies of the initial latex particles. The final powder resulting from this preparative process was checked for MW integrity by GPC and had the same MW distribution as initial homopolymers.

Disk samples for SANS experiments were prepared in molds held in a hot press for 30 min at 107–115 °C and (5–7) × 10^6 Pa. These conditions were chosen, after trial-and-error experimentation, to produce transparent samples with minimum exposure to high temperatures where PSH/PSD interdiffusion could occur. Sample disks were 1.3 cm in diameter and 0.07 cm thick. Completely mixed samples were prepared by annealing disks at 180 °C for 30 min. Homogeneous 50 wt % specimens were prepared by molding disks containing the solvent-mixed powder. The material used in this preparation was obtained from the nonsolvent precipitation of a benzene solution containing both PSH and PSD.

Annealing and SANS Measurements. The measurements were performed with the SANS facilities at the Oak Ridge National Laboratory. SANS results from a short flight path (6.89 m) were used to establish reproducibility of replicate unannealed samples and to establish appropriate annealing times at various temperatures. Thermal annealing was done in an oven at the reactor site. To prevent sample distortion during heating, the sample disks were enclosed in a small steel ring, covered on both sides, and weighted during annealing. Sample thickness and SANS transmission were measured before and after thermal annealing. All specimens were visually translucent/transparent. Scattering from homogeneous samples, prepared from lattices containing PSH and PSD, showed no evidence of void scattering at low Q.

Data on 68 000 MW polystyrene, reported in this paper, were obtained on samples annealed at 130 ± 2 °C for 300–1800 s. A variety of reproducible fully annealed specimens were used as described in the text.

The major diffusion results were obtained with a 16.5-m flight path, a neutron wavelength of 4.75×10^{-8} cm, and source/sample slit diameters of 2.0 and 1.0 cm, respectively. A 8.0-cm beam stop was used. In this configuration, useful SANS data are obtained over the range $4.0 \times 10^5 < Q < 3.5 \times 10^6$ cm^{-1}. The polymer SANS results were referenced to a standard aluminum specimen and then expressed in terms of absolute scattering intensity. Incoherent scattering corrections were made with SANS measurements on 100% PSH. These corrections were small, amounting to a few percent over scattering angles of primary interest.

Analysis of Experimental Results

For a system initially composed of randomly mixed clusters of protonated and deuteriated polymers, Summerfield and Ullman[1] show that $I(Q,t)$, the SANS intensity after annealing time t, can be expressed

$$I(Q,t) = I(Q,0) \exp(-2DQ^2 t) + a(t) I(Q,\infty) \qquad (1)$$

where $I(Q,0)$ and $I(Q,\infty)$ are the scattering intensities from unannealed and fully annealed samples respectively. D, the diffusion coefficient, is presumed to be a constant. The factor $a(t) = 1 - \alpha(0,t)$, where $\alpha(0,t)$ is the normalized integral of a radial correlation function, $\gamma(R,0)$, describing segregated regions in the unannealed sample at time $t = 0$

$$\alpha(0,t) = (8\pi Dt)^{-3/2} \int_0^\infty \gamma(R,0) \exp(-R^2/8Dt) \, dR \qquad (2)$$

By definition, $\alpha(0,\infty) = 0$ and $\alpha(\infty) = 1$ for homogeneous samples at infinite annealing time.

Two effects occur simultaneously during sample annealing. The scattering contribution from the first term in eq 1 decreases with time owing to the factor $\exp(-2DQ^2 t)$. Concurrently, the contribution from the second term increases as $a(t)$ goes from 0 to 1. In the high-Q

region, the first term quickly becomes vanishingly small and $a(t_1)$ can be determined from the ratio of scattering intensities at times $t = t_1$ and $t = \infty$, respectively. In practice, data from many Q values are available for determination of $a(t_1)$, so that this experimental parameter is known with high precision. $I(Q,\infty)$ is the single-chain scattering factor, whose intensity and functional form are known from experiment at $t = \infty$ as well as from theory[11]

$$I(Q,\infty) = c_0(2/u^2) \{\exp(-u) + u - 1\} \qquad (3)$$

where $u = (QR_g)^2$ and c_0 is a known proportionality constant determined by molecular and instrumental parameters. Consequently, one can subtract $a(t_1)I(Q,0)$ from experimental data to obtain $F(Q,t_1) = I(Q,0) \exp(-2DQ^2t_1)$. We note in passing that $I(Q,\infty)$ is effectively zero for binary metals over the Q region used in bulk polymer SANS experiments (Figure 1).

When diffusion is *independent* of Q and t, diffusion coefficients can be obtained from

$$D = -0.5\{d\ln (F(Q,t)/F(Q,0))/d(Q^2t)\} \qquad (4)$$

Q^2 and t are equivalent experimental variables in this representation. Therefore, for a particular sample and annealing time, one can optimize the determination of the experimental diffusion coefficients by combining data at several different Q values and annealing times. In practice, it is useful to compute D values from least-squares slopes of $\ln (F(Q,t)/F(Q,0)) - (Q^2t)$ plots.

Equation 4 is invalid whenever diffusion depends on Q and/or t. Least-squares analysis then yields an average of different D values. In order to investigate possible Q- or t-dependent effects, we computed diffusion coefficients D_t from constant-time measurements as

$$D_t = -0.5\{d\ln (F(Q,t)/F(Q,0))/d(Q^2)\}_t/t \qquad (5)$$

and diffusion coefficients D_Q from constant-Q measurements as

$$D_Q = -0.5\{d\ln (F(Q,t)/F(Q,0))/dt\}_Q/Q^2 \qquad (6)$$

Specifically, we looked for systematic variations of D_t with time, for systematic variations of D_Q with Q, and for systematic curvature in both plots.

Diffusion coefficients can also be determined by analysis of $a(t)$. This method was used by Bartels et al.[9] in SANS diffusion studies of bulk protonated/deuteriated polybutadiene. As noted earlier, the evaluation of D values from $a(t)$ requires more precise knowledge of the initial heterogeneity distribution than the analysis given above. Bartels et al.[9] worked with carefully prepared layered structures of protonated and deuteriated polymers in order to satisfy this requirement. We have no experimental knowledge of scattering from our specimens below $Q = 4.0 \times 10^5$ cm^{-1}. Consequently, we used experimental $a(t)$ results only as a rough consistency check of D values obtained by the other method. Agreement, to approximately 1 order of magnitude, seems satisfactory in light of the large uncertainties involved.

Results and Discussion

In performing SANS diffusion experiments, it is convenient to compare data from different samples that have been annealed for various times. Such comparisons are valid only if the heterogeneous starting materials, i.e., the unannealed samples, are shown to be interchangeable. For this reason, we examined sample reproducibility at SANS sample–detector distances of 6.89 and 16.5 m. Fourteen different unannealed samples, prepared from a single batch of protonated/deuteriated polymer, exhibited scattering
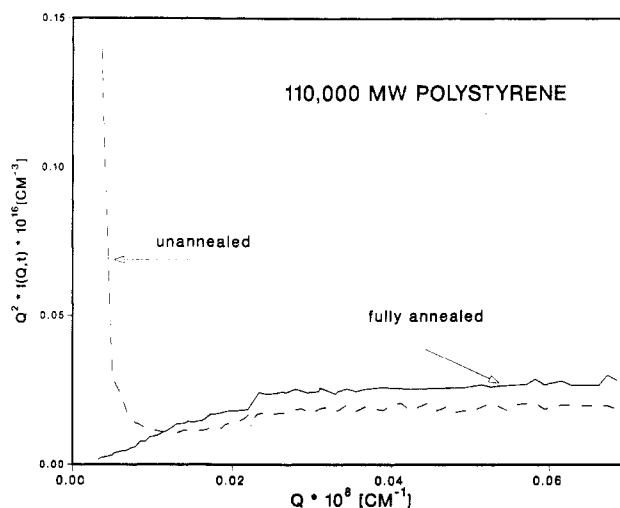
Figure 2. Experimental SANS data for 100 000 MW polystyrene annealed at 120 °C. Results at intermediate annealing times (not shown) fall between these limiting curves. The Kratky representation, plotting $Q^2I(Q)$ vs. Q, emphasizes decreasing and increasing portions of SANS curves with annealing time.

patterns that matched within 10% over the entire Q range at 6.89 m. Scattering from three of these specimens, measured again at 16.5 m, showed similar reproducibility. This reproducibility matched that found in repeated SANS measurements on a single unannealed sample. Larger scattering differences were observed between unannealed samples from different preparations, i.e., different batches, of heterogeneous polymer. For this reason, only specimens taken from the same batch of starting material were used together in diffusion studies.

Bates et al.[12,13] recently reported SANS observations of high-temperature phase separation in bulk specimens containing both protonated and deuteriated polystyrene. This is a high MW effect, not expected to occur with the lower MW polystyrenes used in the present research.[14] For completeness we prepared six 1:1 protonated:deuteriated samples of 110 000 MW polystyrene directly from solution: SANS measurements show characteristic single-chain scattering (vide eq 3), with no indication of heterogeneities of phase separation. The samples were then subjected to various thermal posttreatments designed to promote any latent phase separation. However, none of these heating cycles changed subsequent SANS results beyond the limits of sample reproducibility. These negative results confirm the expectation that phase separation does not occur in 110 000 MW blends of protonated and deuteriated polystyrene. More important, they demonstrate experimentally that spatial uniformity represents equilibrium for the heterogeneous samples of protonated/deuteriated polystyrene. The entire diffusion analysis becomes suspect without this demonstration.

Figure 2 shows representative scattering curves for 110 000 MW polystyrene samples. Note the characteristic decrease in low-Q scattering and concurrent increase in high-Q scattering with annealing time. SANS from unannealed samples varies roughly as

$$I(Q,0) = (c_1R_c^3)/(1 + (QR_c)^2)^2 \qquad (7a)$$

with a radial correlation length, R_c, and

$$c_1 = 8\pi\phi(1 - \phi)(N_A\rho/M_M)^2(a_H - a_D)^2 \qquad (7b)$$

In eq 7b, N_A is Avogadro's number, ρ is the density, M_M is the monomer MW, and a_H and a_D are the neutron
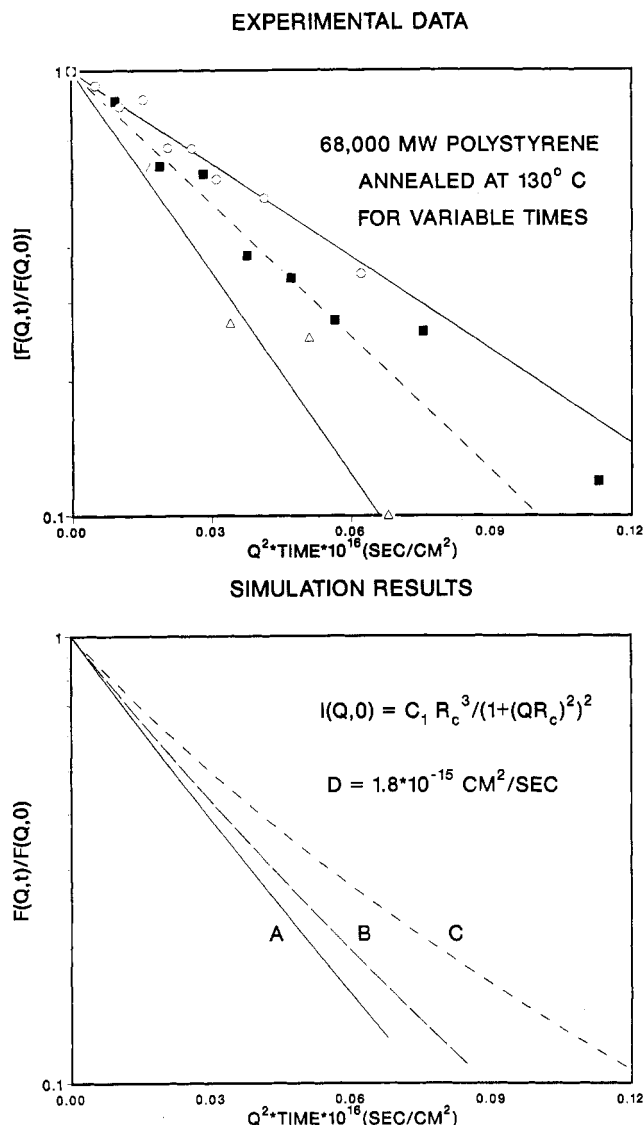
Figure 3. (Top) Decay of experimental SANS with annealing time. Data were taken at constant Q values and various times. Circles, $Q = 4.15 \times 10^5$ cm^{-1}; squares, $Q = 5.60 \times 10^5$ cm^{-1}; triangles, $Q = 7.52 \times 10^5$ cm^{-1}. (Bottom) Decay simulation scattering with annealing time. Intensities computed for fixed scattering angles. Curves A, B, and C correspond to $Q = 4.15 \times 10^5$, 5.60×10^5, and 7.52×10^5 cm^{-1}. $\Delta Q_T = 2.1 \times 10^5$ cm^{-1} was assumed in convolution "smearing" (vide eq 12).

Figure 4. (Top) Decay of experimental SANS with scattering angle (Q^2) at fixed annealing times. Circles, $t = 300$ s; squares, $t = 600$ s; diamonds, $t = 1200$ s; triangles, $t = 1800$ s. (Bottom) Decay of simulation results, at fixed times, with Q^2. Curve A, $t = 300$ s; curve B, $t = 600$ s; curve C, $t = 1200$ s; curve D, $t = 1800$ s. $\Delta Q_T = 2.1 \times 10^5$ cm^{-1} was used in convolution "smearing" (vide eq 12).

cross-sections for the C_8H_8 and C_8D_8 monomer units. The functional form of eq 7a was obtained by Debye et al.[15,16] The match is best in the range 4.0×10^5 cm^{-1} < Q < 1.0×10^6 cm^{-1}. Experimental curves decay more slowly than eq 7a at higher Q values where they exhibit a rough Q^{-2} rather than a Q^{-4}, variation. Batch-to-batch variations of R_c were seen, ranging between 7×10^{-5} and 9×10^{-5} cm. Scattering curves from samples annealed for long times, or for shorter times at 150–180 °C, match SANS results from solution-grown samples.

The first step in the data reduction subtracts $a(t)I(Q,\infty)$ terms from $I(Q,t)$ to form $F(Q,t)$. This introduces no appreciable uncertainty into the subsequent analysis since $a(t)I(0,\infty)$ is relatively small over the range 4×10^5 cm^{-1} < Q < 8×10^5 cm^{-1}, never amounting to more than $0.2I$-$(Q,0)$. The reduced $F(Q,t)$ data were used in plots corresponding to eq 5 and 6 to investigate Q- or time-dependent effects on diffusion. Figures 3 and 4 show reduced data obtained from 68000 MW polystyrene annealed at 130 °C.

Figure 3, showing representative data at three different scattering angles, suggests Q-dependent diffusion coeffi-
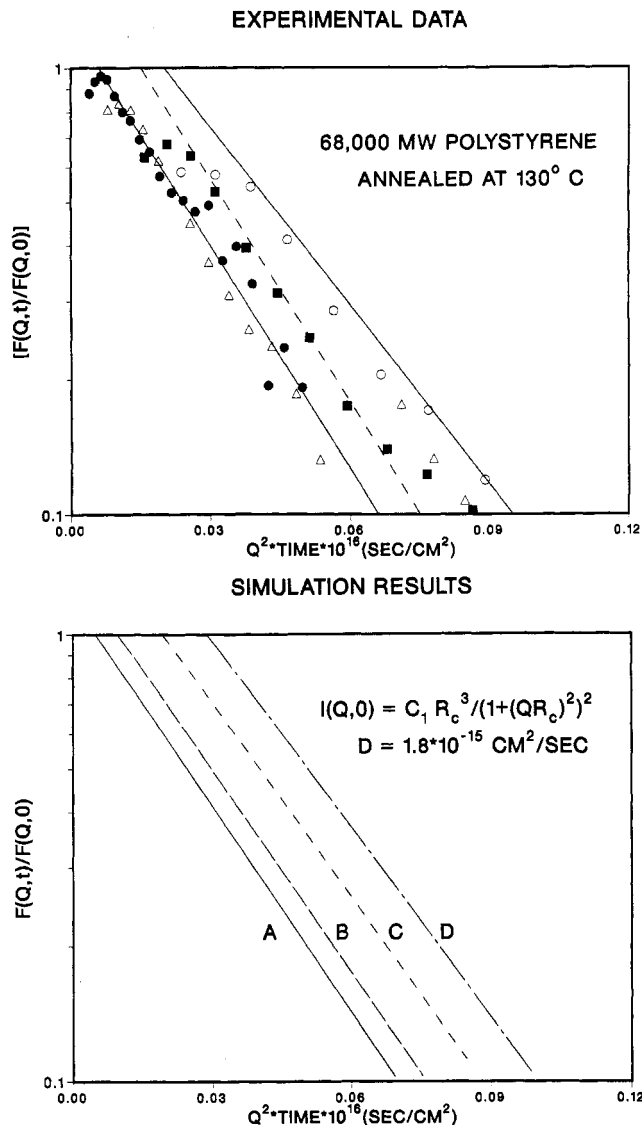
cients: These plots should be collinear if D were constant. These results, together with similar data at intermediate scattering angles, indicate that experimental D values increase by a factor of 2 between $Q = 4.15 \times 10^5$ and 7.98 $\times 10^5$ cm^{-1} (Figure 5), approaching the value $D_Q = 1.8 \times 10^{-15}$ cm^2/s at high Q. The rapid decrease of $\ln F(Q,t)/F(Q,0)$ at higher scattering angles limits the range of these experiments; at higher Q values there are too few reliable points to evaluate meaningful D values. For example, with $D_Q = 1.8 \times 10^{-15}$ cm^2/s, $Q = 1.0 \times 10^5$ cm^{-1}, $\exp(-2DQ^2 t_1)$ decays to 0.34 at our shortest annealing time ($t_1 = 300$ s). It should be noted that this limitation is specimen-dependent. Useful data are readily obtained at higher Q values with samples having smaller diffusion coefficients.

Figure 4 shows experimental data on the same system taken at four annealing times and plotted as a function of Q^2. For constant Dt, these plots should be collinear and extrapolate to unity at $Q^2 = 0$. Consequently, the data suggest Q-dependent or time-dependent diffusion coefficients. Examination of these graphs and of similar Q^2 plots for other annealing times (not shown) indicates the experimental Q^2 slope is fairly constant with annealing time,
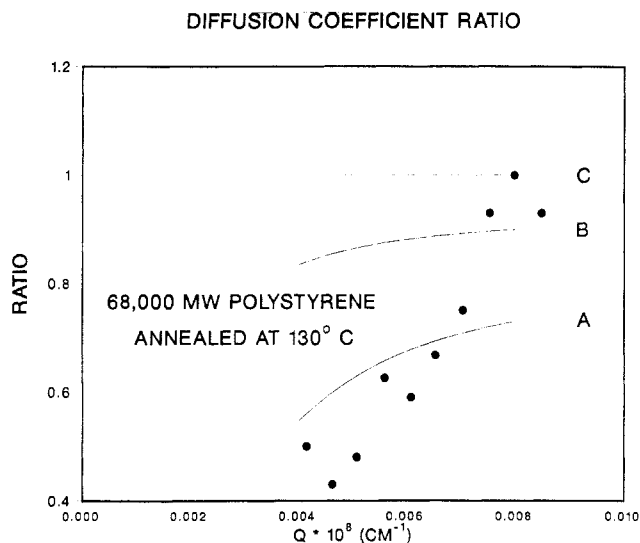
DIFFUSION COEFFICIENT RATIO

Figure 5. Q dependence of diffusion coefficients. Experimental points, diamonds, obtained by least-squares determination of (dln $(F(Q,t)/F(Q,0))/dt)_Q$ slopes, and referenced to $D = 1.8 \times 10^{-15}$ cm²/s. Solid line from simulation with $D = 1.8 \times 10^{-15}$ cm²/s, $I(Q,0) = c_1 R_c^3/(1 + (QR_c)^2)^2$, $R_c = 9.0 \times 10^{-5}$ cm. Curves A, B, and C correspond to $\Delta Q_T = 2.1 \times 10^5$, 1.0×10^5, and 1.0×10^3 cm⁻¹, respectively. Comparison of curves and points illustrates qualitative similarities not quantitative fit.

but the $Q^2 = 0$ intercept becomes substantially larger than unity at longer annealing times.

Scattering experiments on binary metal systems[6-8] exhibit Q-dependent diffusion coefficients. These are attributed to higher order corrections to Fick's law that operate over extremely small distances. Similar departures from Fick's law would not be totally unexpected in polymer diffusion studies made over distances comparable to the radius of gyration.

Instrumental effects provide an alternative interpretation of these observations. The following section describes simulation results showing that a distribution of Q values, i.e., "smearing effects", leads to apparent Q-dependent diffusion coefficients. It is important to note that an instrumental explanation requires a fwhm ΔQ_T of roughly 2.1×10^5 cm⁻¹ to produce the $D(Q)$ variation seen experimentally for 68000 MW polystyrene. As shown in Figure 5, smaller ΔQ_T values will not account for our observations.

"Smearing effects" undoubtedly make a substantial contribution to the experimentally observed $D(Q)$ in 68000 MW polystyrene at 130 °C. Indeed, for this polymer at this temperature, smearing can account for all of this effect. We have less extensive data, obtained at lower temperatures and on polystyrene samples of higher molecular weights, where the experimental Q variation of D seems too large to be explained completely by smearing.

Effect of a Q Distribution upon SANS Diffusion Measurements

Analysis of SANS data presupposes 1:1 correspondence between (a) scattering by the sample at wavevector Q_0 and (b) scattering intensity measured at a specific position on the area detector. This supposition is largely, but not completely, true. For example, Mildner et al.[17] cite three factors that cause detector intensity to be "smeared" by a distribution of Q values: (1) distribution of neutron energies; (2) source–sample–detector geometry; (3) digitization characteristics of the area detector. They showed that these factors are equivalent to a distribution of Q values incident on the sample. Mildner et al.[17] developed computational methods for estimating ΔQ_T, the fwhm deviation of Q about an average value of Q_0, in terms of

instrumental parameters. ΔQ_T values, computed by this procedure, were validated by experiments at the University of Missouri Neutron Scattering Facility.[17]

Equations 8 and 9 modify expressions from Mildner et al.[17] Numerical values, given in parentheses, refer to instrumental quantities used in our experiments at Oak Ridge National Laboratory.[18]

$$\Delta Q_T^2 = \Delta Q_\lambda^2 + \Delta Q_g^2 + \Delta Q_d^2 \qquad (8)$$

Three factors govern ΔQ_T^2, the total instrumental broadening function. The first of these is the neutron energy distribution, given by $\Delta Q_\lambda^2 = 3.6 \times 10^{-3} Q_0^2$. A second factor is the source–sample–detector geometry, ΔQ_g^2, given by

$$\Delta Q_g^2 = (k_0^2/2)(R_1/L_1)^2 + R_2^2((1/L_1) + (1/L_2))^2 = 2.3 \times 10^{10} \text{ (cm}^{-2}) \quad (9)$$

where $k_0 = (2\pi/\lambda) = 1.322 \times 10^8$ cm⁻¹, L_1 and L_2 are the source–sample (760 cm) and sample–detector (1650 cm) distances, and R_1 and R_2 are the source (1.0 cm) and sample (0.5 cm) apertures. The third factor, ΔQ_d^2, arises from digitization broadening and is given by

$$\Delta Q_d^2 = k_0^2(\Delta D)^2/L_2^2 = 2.0 \times 10^{10} \text{ (cm}^{-2}) \qquad (10)$$

where $\Delta D = 1.75$ cm is the root-mean-square cell dimension. Summing these contributions, one obtains

$$\Delta Q_T^2 = 3.6 \times 10^{-3} Q_0^2 = 4.3 \times 10^{10} \text{ (cm}^{-2}) \qquad (11)$$

or $\Delta Q_T \sim 2.1 \times 10^5$ cm⁻¹ over the range 4×10^5 cm⁻¹ $< Q < 10 \times 10^5$ cm⁻¹. We used this value to simulate ΔQ_T effects on SANS diffusion experiments. Scattering intensities at the detector, $I_d(Q,t)$, were computed by convolution

$$I_d(Q_0,t) = \int_{-\infty}^{\infty} I_S(Q,t) \exp\{-2.77((Q - Q_0)/\Delta Q_T)^2\} \, d(Q - Q_0) \quad (12)$$

The scattering function of the sample, $I_S(Q,t)$, was taken to have the form

$$I_S(Q,t) = \{c_1 R_c^3/(1 + (QR_c)^2)^2\} \exp(-2DQ^2 t) \quad (13)$$

Simulation involved numerical integration of eq 12 between limits of $\pm(1.5 \Delta Q_T)$. $I_d(Q_0,t)$ and $I_s(Q_0,t)$ differ by less than 10% when $\Delta Q_T/Q_0$ is less than 0.1. Significant differences between $I_d(Q_0,0)$ and $I_S(Q_0,Q)$ arise at larger $\Delta Q_T/Q_0$ values. Differences also increase with the d(I_S-$(Q,0)$)/dQ slope. Convolution causes intense sample scattering at $Q < Q_0$ to contribute to detector intensities at Q_0, making $I_d(Q_0,t) > I_S(Q_0,t)$. The largest $(I_d(Q_0,t)/I_S(Q_0,t))$ ratios occur at small Q_0, where $\Delta Q_T/Q_0$ is greatest. At higher scattering angles, where $\Delta Q_T/Q_0 < .1$, $I_d(Q_0,t) \sim I_S(Q_0,t)$.

Similar arguments pertain to SANS diffusion measurements. Owing to (a) the strong decrease of $I(Q,0)$ with increasing Q and (b) the strong decrease of $\exp(-2DQ^2 t)$ with increasing Q, contributions from $Q < Q_0$ dominate the integral in eq 12. This effectively shifts the nominal Q_0 to a smaller effective value and slows the decay of (dln $(F(Q,t)/F(Q,0))/dt)_Q$ plots. Figure 3 (bottom) shows simulation data, obtained with different Q_0 values, plotted as ln $(I_d(Q_0,t)/I_d(Q_d,0))$ vs. $(Q_0^2 t)$. If one calculates diffusion coefficients from the slope of these plots (vide eq 6), one encounters *apparent Q_0-dependent D values* (Figure 5). D values calculated from low Q_0 (and high $\Delta Q_T/Q_0$) data are smaller than D values used as input to the simulation; however, the input D value is approached asymptotically at higher Q_0 values. Some curvature appears in plots of

simulated data for large $(\Delta Q_T/Q_0)$ values. Given the inherent experimental scatter i reduced intensity–time plots, it is uncertain whether curvature can be identified unambiguously in any of our data.

Smearing effects take a different form if one analyses diffusion via $\ln (I_d(Q,t)/I_d(Q,0))_t - Q^2$ plots at fixed annealing times (vide eq 5). Simulation leads to curves with slopes corresponding to input D values but intercepts at $Q_0 = 0$ larger than unity (Figure 4 (bottom)). Experimental (Figure 4 (top)) and simulation results can again be attributed to effective reduction of the nominal Q_0 values bought about by the convolution.

Several numerical algorithms have been developed for "desmearing" experimental scattering data.[19-21] Attempts to use Oak Ridge "desmearing routines" with the present data were unsuccessful owing to the large R_c: the routines did not converge.

Operationally, we found that experimental and simulation intensity results form collinear plots of $\ln (F(Q,t)/F(Q,0))$ vs. $((Q_0 - 0.5 \, \Delta Q_T)^2 t)$—rather against $(Q_0^2 t)$ as in eq 4-6. This procedure was an attempt to recast smearing/convolution effects in terms of an effective scattering angle, Q_{eff}, somewhat less than Q_0. The variable $Q_{eff} = (Q_0 = 0.5\Delta Q_T)$ is arbitrary, since the best match depends on the (dI/dQ) slope. Use of this approximation suggests that diffusion coefficients from smeared data vary as $D(\text{true})/(1 + \Delta Q_T/Q_0))^2$; which fits simulated results fairly well (Figure 5).

Conclusion

This research considers SANS diffusion studies of bulk polymers. As pointed out in the Introduction, these measurements are an application of well-known metallurgical experiments to polymers. However, the adaptation from metals to macromolecules is not trivial: Sample annealing of (monomeric) metals creates increasing and decreasing scattering in well-separated regions of Q space, and data analysis is straightforward. Macromolecular dimensions produce overlap between growing and decaying portions of scattering curves. The recent Summerfield–Ullman calculation[1] affords a mechanism for isolating these components. The present results validate this analysis.

Several other new experimental methods for studying diffusion in bulk polymers have been reported recently. These include (a) infrared microdensitrometry;[3] (b) photochromic holography;[2] (c) Rutherford backscattering.[4] Owing to the limited accessibility of SANS instrumentation, each of these methods is probably faster and more convenient for routine diffusion measurements than the SANS method described here. However, SANS diffusion measurements have two unique features which may be crucial in special cases.

First, it follows from the scattering law and the neutron wavelength, $\lambda \sim (1-5) \times 10^{-8}$ cm, that SANS experiments view diffusion over distances of $10^{-5}-10^{-7}$ cm. These distances are less than or comparable to the macromolecular radius of gyration. This is of interest in itself. Furthermore, it follows from the Fickian relation $D = \langle x^2 \rangle /2t$ that SANS measures extremely slow diffusion coefficients over

convenient experimental time scales. For example, our experimental diffusion coefficient for 68 000 MW polystyrene at 130 °C, 1.8×10^{-15} cm²/s, is among the smallest polymer diffusion coefficients reported; however, it is considerably larger than the $D \sim 10^{-20}$ cm²/s reported for Au–Cu in 1940.[5]

Second, SANS measurements at different scattering angles afford independent determinations of diffusion coefficients. These values can be compared with one another to probe the presence, or absence, of Q-dependent; i.e., space-dependent, diffusion. Instrumental effects, such as "smearing", complicate this comparison and limit the minimum Q dependence that can be identified unambiguously. However, we are unaware of other diffusion experiments that allow such comparisons to be made at all.

References and Notes

(1) Summerfield, G. C.; Ullman, R. *Macromolecules* **1987**, *20*, 401.
(2) Antonietti, M.; Coutandin, J.; Gritter, R.; Sillescu, H. *Macromolecules* **1984**, *17*, 798.
(3) Klein, J.; Fletcher, D.; Fetters, L. J. *Faraday Symp. Chem. Soc.* **1983**, No. 18, 159; *Nature (London)* **1983**, *304*, 526 and references therein.
(4) Kramer, E. J.; Green, P.; Palmstrom, C. *Polymer* **1984**, *25*, 473.
(5) DuMond, J.; Youtz, J. P. *J. Appl. Phys.* **1940**, *11*, 357.
(6) Philofsky, E. M.; Hilliard, J. E. *J. Appl. Phys.* **1969**, *40*, 2198.
(7) Cook, H. E.; Hilliard, J. E. *J. Appl. Phys.* **1969**, *40*, 2191.
(8) See, for example: Hilliard, J. E., In *Phase Transformations*: Aaronson, H. I., Ed.; Chapman and Hall: London, 1970; pp 538 ff.
(9) Bartels, C. R.; Crist, B.; Graessley, W. W. *J. Polym. Sci., Polym. Lett. Ed.* **1983**, *21*, 495; *Macromolecules* **1984**, *17*, 2702.
(10) Hashimoto, T.; Tsukahar, Y.; Kawai, H. *Macromolecules* **1981**, *14*, 708.
(11) Zimm, B. H. *J. Chem. Phys.* **1948**, *19*, 1093.
(12) Bates, F. S.; Wignall, G. D.; Koehler, W. C. *Phys. Rev. Lett.* **1985**, *22*, 2425.
(13) Bates, F. S.; Wignall, G. D. *Macromolecules* **1986**, *19*, 932.
(14) Buckingham, A. D.; Hentschel, H. G. E. *J. Polym. Sci., Polym. Phys. Ed.* **1980**, *18*, 853.
(15) Debye, P.; Bueche, A. M. *J. Appl. Phys.* **1949**, *20*, 518.
(16) Debye, P.; Anderson, H. R.; Brumberger, H. *J. Appl. Phys.* **1957**, *28*, 679.
(17) Mildner, D. F. R.; Berliner, R.; Pringle, O. A.; King, J. S. *J. Appl. Crystallogr.* **1981**, *14*, 370.
(18) Ramakrishnan, V. *J. Appl. Crystallogr.* **1985**, *18*, 42.
(19) Glatter, O. *J. Appl. Crystallogr.* **1977**, *10*, 415.
(20) Muller, J. J.; Damaschun, G. *J. Appl. Crystallogr.* **1979**, *12*, 267.
(21) Moore, P. B. *J. Appl. Crystallogr.* **1980**, *13*, 168.